

Lecture Notes on Fluid Dynamics
(1.63J/2.21J)
by Chiang C. Mei, 2002

6-7double-diff.tex

May 10, 2003

6.7 Thermohaline instability in a porous layer -doubly-diffusive instability

[Refs]: Porous Media:

Cheng, Ping, 1978. Heat Transfer in Geothermal Systems, *Advances in Heat Transfer*, 14, 1-105.

Nield & Bejan, *Convection in Porous Media* .

O. M. Phillips, 1991 *Flow and Reactions in Permeable Rocks*, Cambridge Univ. P.

Imhoff & Green 1988, Experimental investigation of double diffusive ground water fingers. *J. Fluid Mech.* , 188, 363-382.

R. W. Griffiths, (1981) Layered double-diffusive convection in porous media. *J. Fluid Mech.* 102, 221-248.

Oceanography:

M.E. Stern (1960) The salt fountain and thermohaline convection *Tellus* 12, 172-175.

J. S. Turner, (1973) *Buoyancy Effects in Fluids* Cambridge.

A. Brandt & H. J. S. Fernando: *Double-diffusive Convection* Geophysics Monograph 94, 1995, AGU.

Raymond Schmitt, 1994. Double diffusion in oceanography, *Annual Rev. Fluid Mech.* 255-286.

P. K. Kundu, (1990) *Fluid Mechanics* , Academic.

In Salton Sea geothermal field of Imperial Valley, California, the temperature in the hotwater reservoir can be $360^{\circ}C$. Salinity in groundwater is as high as 2.5×10^5 ppm. Due to sharp contrast of thermal and salt diffusivities ($\kappa_T \sim 1.5 \times 10^{-7} m^2/s$, $\kappa_S \sim 1.5 \times 10^{-9} m^2/s$), convection can result from instability. This is called thermohaline convection.

A very similar mechanism was discovered earlier in oceanography, by Melvin Stern (1960). This is another example where essentially the same physics arises in vastly different contexts.

6.7.1 Heuristic picture

Monotone instability

Consider a fluid lighter at the top and denser at the bottom, with T and C shown in Figure 6.7.1. so that $dT/dz, dC/dz > 0$.

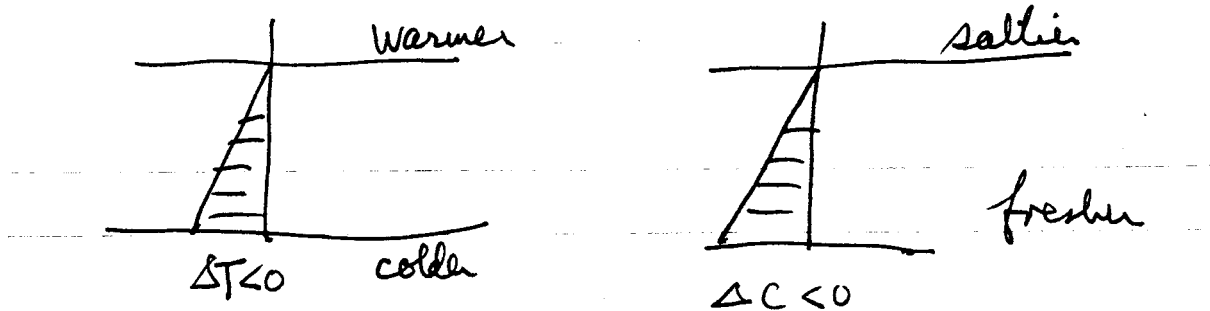


Figure 6.7.1: Salinity and temperature profiles favoring monotonic instability in a porous medium

Let a fluid parcel rise from z to $z + \Delta z$. Because the thermal diffusivity κ_m is much greater than the mass diffusivity of salt, κ_s , the rising water parcel absorbs heat much more quickly than it absorbs salt. Hence, it can become lighter than the surrounding fluid and continue to rise. If a fluid parcel drops by Δz , the faster heat loss can make it heavier than its surrounding fluid and sinking continues. Thus the fluid system can be unstable.

Oscillatory instability Consider a cold and fresh water lying over a warm and salty water. Assume that the fluid density decreases with height. The profiles of T and C are shown in figure 6.7.2 so that $dT/dz, dC/dz < 0$. A lighter fluid parcel accidentally moved up by Δz

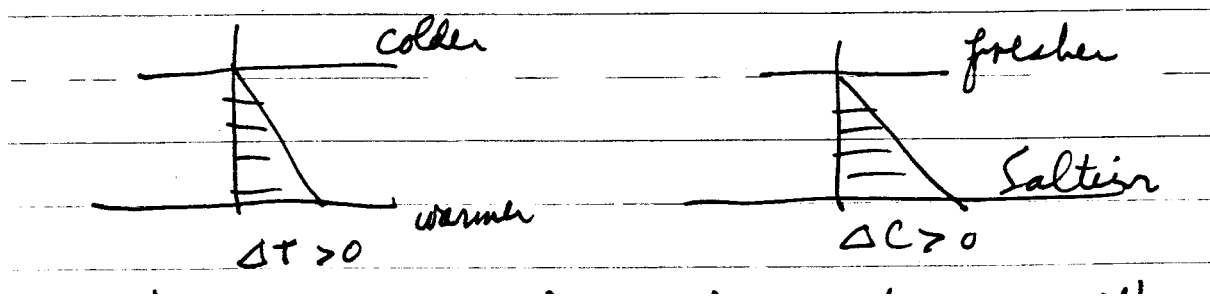


Figure 6.7.2: Salinity and temperature profiles favoring oscillatory instability in a porous medium

will cool off quickly while losing little salt. Hence, it will come down, resulting in oscillations.

We shall describe the mathematics of the initial instability theory.

6.7.2 Governing equations

Conservation of Fluid Mass:

$$\nabla \cdot \vec{u} = 0 \quad (6.7.1)$$

Conservation of fluid momentum:

$$0 = -\nabla p - \frac{\mu}{k} \mathbf{u} + \rho_f \vec{g} \quad (6.7.2)$$

Energy:

$$\sigma \frac{\partial T}{\partial t} + \mathbf{u} \cdot \nabla T = \kappa_m \nabla^2 T, \quad (6.7.3)$$

$$\sigma = \frac{(\rho c)_{fluid}}{(\rho c)_{mix}}$$

Conservation of Salinity :

$$n \frac{\partial C}{\partial t} + \mathbf{u} \cdot \nabla C = \kappa_s \nabla^2 C \quad (6.7.4)$$

Equation of state:

$$\rho_f = \rho_0 [1 - \beta (T - T_0) + \beta_s (C - C_0)] \quad (6.7.5)$$

Note the sign difference of thermal expansion coefficient and salinity.

Static equilibrium:

$$\mathbf{u} = 0 \quad (6.7.6)$$

$$\begin{aligned} T_s &= T_0 + \Delta T \left(1 - \frac{z}{H}\right) \\ C_s &= C_0 + \Delta C \left(1 - \frac{z}{H}\right) \end{aligned} \quad (6.7.7)$$

$$P_s = P_0 - \rho_0 g \left[z - \frac{\beta}{2} \Delta T \left(2z - \frac{z^2}{H}\right) + \frac{\beta_s}{2} \Delta C \left(2z - \frac{z^2}{H}\right) \right] \quad (6.7.8)$$

6.7.3 Perturbed flow

Let $\mathbf{u} = \mathbf{u}'$ be the velocity disturbance, and let

$$T = T_s + T', \quad p = p_s + p', \quad C = C_s + C'$$

The perturbations must satisfy:

$$\nabla \cdot \mathbf{u}' = 0 \quad (6.7.9)$$

$$0 = -\nabla p' - \frac{\mu}{k} \mathbf{u}' - \rho_0 (\beta T' - \beta_s C') \mathbf{g} \quad (6.7.10)$$

$$\sigma \frac{\partial T'}{\partial t} - w' \frac{\Delta T}{H} = \kappa_m \nabla^2 T' \quad (6.7.11)$$

$$n \frac{\partial C'}{\partial t} - w' \frac{\Delta C}{H} = \kappa_s \nabla^2 C' \quad (6.7.12)$$

6.7.4 Normalization

$$\begin{aligned}
(x, y, z) &= H(x^*, y^*, z^*), & \nabla &= \frac{\nabla^*}{H} \\
t &= \frac{\sigma H^2}{\kappa_m} t^*, & \mathbf{u}' &= \frac{\kappa_m}{H} \mathbf{u}^* & T' &= |\Delta T| T^* \\
C' &= |\Delta C| C^* & p' &= \frac{\mu \kappa_m}{k} p^*
\end{aligned} \tag{6.7.13}$$

The dimensionless equations, are, with * omitted for brevity,

$$\nabla \cdot \mathbf{u} = 0 \tag{6.7.14}$$

$$-\nabla p - \mathbf{u} + \left(Ra T - \frac{Ra_s}{Le} C \right) \mathbf{e}_3 = 0 \tag{6.7.15}$$

$$\frac{\partial T}{\partial t} - w = \nabla^2 T \tag{6.7.16}$$

$$Le \left(\mathcal{N} \frac{\partial C}{\partial t} - W \right) = \nabla^2 C, \tag{6.7.17}$$

where

$$Ra = \frac{g \beta k H \Delta T}{\nu \kappa_m} = \text{thermal Rayleigh No.} \tag{6.7.18}$$

$$Ra_s = \frac{g \beta_s k H \Delta C}{\nu \kappa_s} = \text{salinity Rayleigh No.} \tag{6.7.19}$$

$$Le = \frac{k_m}{k_s} = \text{Lewis No.} \tag{6.7.20}$$

$$\mathcal{N} = \frac{n}{\sigma} \tag{6.7.21}$$

$$\cdot \tag{6.7.22}$$

Note that

$$Ra_s = Ra N Le, \tag{6.7.23}$$

where

$$N = \frac{\beta_s \Delta C}{\beta \Delta T} \tag{6.7.24}$$

can be either positive or negative. Taking curl of Eqn. (6.7.15)

$$\nabla \times \mathbf{u} = Ra \{ (T_y - NC_y) \mathbf{e}_1 - (T_x - NC_x) \mathbf{e}_2 \}. \tag{6.7.25}$$

Taking curl of the above and using $\nabla \cdot \mathbf{u} = 0$

$$\nabla^2 \mathbf{u} = -Ra \{ (T_{xz} - NC_{xz}) \mathbf{e}_1 + (T_{yz} - NC_{yz}) \mathbf{e}_2 \tag{6.7.26}$$

$$- [(T_{xx} + T_{yy}) - N (C_{xx} + C_{yy})] \mathbf{e}_3 \}. \tag{6.7.27}$$

The z component is

$$\nabla^2 w = Ra (\nabla_2^2 T - N \nabla_2^2 C), \quad \nabla_2 = \frac{\partial^2}{\partial x^2} + \frac{\partial^2}{\partial y^2} \quad (6.7.28)$$

with the boundary conditions,

$$w = T = C = 0, \quad \text{at } z = 0, 1. \quad (6.7.29)$$

Consider sinusoidal disturbances

$$\begin{pmatrix} W \\ T \\ C \end{pmatrix} = \begin{pmatrix} \tilde{W} \\ \tilde{T} \\ \tilde{C} \end{pmatrix} e^{-i\omega t + i\ell x + imy} \quad (6.7.30)$$

From Eqn. (6.7.28)

$$(D^2 - a^2) \tilde{W} = -a^2 Ra (\tilde{T} - N \tilde{C}) \quad (6.7.31)$$

From Eqn. (6.7.16)

$$-i\omega \tilde{T} - \tilde{W} = (D^2 - a^2) \tilde{T} \quad (6.7.32)$$

From Eqn. (6.7.17)

$$(-i\omega(n/\sigma) \tilde{C} - \tilde{W}) Le = (D^2 - a^2) \tilde{C} \quad (6.7.33)$$

where

$$D = \frac{d}{dz} \quad \text{and} \quad a^2 = \ell^2 + m^2$$

The boundary conditions are

$$\tilde{W} = \tilde{T} = \tilde{C} = 0, \quad z = 0, 1 \quad (6.7.34)$$

We can eliminate \tilde{T} and \tilde{C} by applying the operator

$$(D^2 - a^2 + i\omega) (D^2 - a^2 - i\omega(n/\sigma) Le)$$

on Eqn. (6.7.31) and using Eqns. (6.7.32) and (6.7.33), to get

$$\begin{aligned} & (D^2 - a^2 + i\omega) (D^2 - a^2 + i\omega(n/\sigma) Le) (D^2 - a^2) \tilde{W} \\ & - a^2 Ra (D^2 - a^2 + i\omega(n/\sigma) Le) \tilde{W} + a^2 Ra_s (D^2 - a^2 + i\omega) \tilde{W} = 0 \end{aligned} \quad (6.7.35)$$

The boundary conditions are

$$\tilde{W} = 0 \quad (6.7.36)$$

$$D^2 \tilde{W} = 0 \quad \text{see (6.7.31)} \quad (6.7.37)$$

$$D^4 \tilde{W} = 0 \quad \text{see (6.7.32) \& (6.7.33)} \quad (6.7.38)$$

Similarly one can show that $D^{2n}W = 0$ on the boundaries. Assume the solution

$$W = \sin j\pi z \quad (6.7.39)$$

we get from Eqn. (6.7.35) the eigenvalue condition,

$$\begin{aligned} & - (j^2\pi^2 + \omega^2) (j^2\pi^2 + a^2 - i\omega) (j^2\pi^2 + a^2 - i\omega\mathcal{N}) \\ & + a^2 Ra [j^2\pi^2 + a^2 - i\omega\mathcal{N}] - a^2 Ra_s [j^2\pi^2 + a^2 - i\omega] = 0 \end{aligned} \quad (6.7.40)$$

where

$$\mathcal{N} = \frac{n}{\sigma} Le \quad (6.7.41)$$

In general ω is complex. At the threshold of instability, $\omega = \text{real}$. From the the real part of (6.7.40):

$$Ra - Ra_s = \frac{(j^2\pi^2 + a^2)^2}{a^2} - \frac{\mathcal{N}}{a^2}\omega^2 \quad (6.7.42)$$

From the imaginary part of Eqn. (6.7.40):

$$\omega [\mathcal{N}(\sigma Ra) - Ra_s] = \omega \left[\frac{(j^2\pi^2 + a^2)^2}{a^2} (1 + \mathcal{N}) \right] \quad (6.7.43)$$

Both these equations represent instability thresholds and must hold for real ω .

6.7.5 Monotonic instability

There is no oscillation and the real part of ω is also zero. It follows from (6.7.42) that

$$Ra - Ra_s = \frac{(j^2\pi^2 + a^2)^2}{a^2} \quad (6.7.44)$$

When there is no salinity, $\Delta C = 0$ and only temperature variation in the background, it is necessary that $\Delta T > 0$ (or $\sigma Ra > 0$, warmer water is at the bottom) for instability. Similarly, when there is no temperature variation ($\Delta T = 0$) and only salinity variation, $\Delta C < 0$ (or $Ra_s < 0$) is necessary for instability. With both effects present, we expect that $Ra - Ra_s > 0$ corresponds to instability. In particular to find the lowest threshold of instability as a function of a , we take $j = 1$, we take

$$\frac{\partial}{\partial a^2}(Ra - Ra_s) = 0 \quad \rightarrow a^2 = \pi^2 \quad (6.7.45)$$

Therefore, the lowest threshold for $\omega = 0$ gives

$$\boxed{Ra - Ra_s = 4\pi^2} \quad (6.7.46)$$

which is a straight line in Figure 6.7.3. The region of instability but lie to the right of this line.

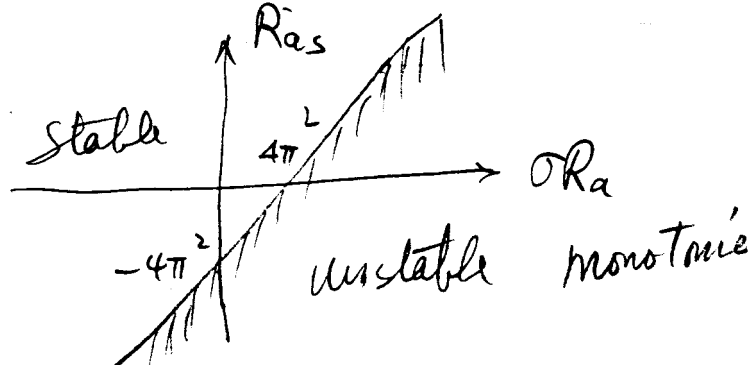


Figure 6.7.3: Domains of monotonic stability and instability

6.7.6 Oscillatory instability

We now assume that the real part of $\omega \neq 0$. From Eqn. (6.7.43)

$$\mathcal{N}Ra - Ra_s = \frac{(j^2\pi^2 + a^2)^2}{a^2}(1 + \mathcal{N})$$

The lowest threshold of oscillatory instability is at : $j = 1, a^2 = \pi^2$

$$\boxed{\mathcal{N}Ra - Ra_s = 4\pi^2(1 + \mathcal{N})} \quad (B) \quad (6.7.47)$$

If $\mathcal{N}Ra - Ra_s > 4\pi^2(1 + \mathcal{N})$, oscillatory instability occurs. The frequency of oscillation ω is given by Eqn. (6.7.42)

$$\frac{\mathcal{N}\omega^2}{\pi^2} = 4\pi^2 - (Ra - Ra_s) \quad (6.7.48)$$

Since ω is real, we must have

$$\boxed{4\pi^2 \geq Ra - Ra_s}, \quad (A) \quad (6.7.49)$$

for instability. The equality sign is one boundary.

The second boundary is defined by Eqn. (6.7.47) which is a straight line that intersects with Eqn. (6.7.49) at

$$(Ra)_c = \frac{4\pi^2\mathcal{N}}{\mathcal{N} - 1} \quad \text{and} \quad (Ra_s)_c = \frac{4\pi^2}{\mathcal{N} - 1}. \quad (6.7.50)$$

Example: $\mathcal{N} = 2$

$$(Ra)_c = 8\pi^2, \quad (Ra_s)_c = 4\pi^2$$

Hence the wedge-like region (doubly hatched) of oscillatory instability is in the first quadrant of Figure 6.7.4.

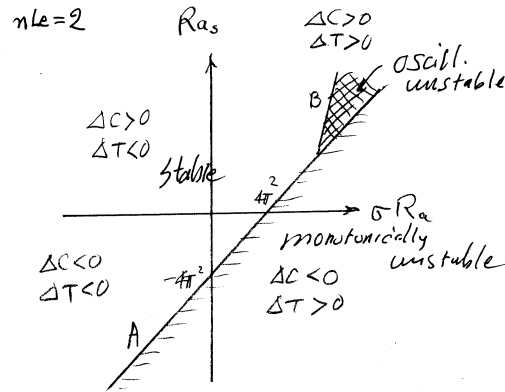


Figure 6.7.4: Domains of stability/instability for $nLe = 2$.

Example: $\mathcal{N} = 1/2$

The second boundary intersects with the first at

$$(Ra)_c = -4\pi^2 \quad (Ra_s)_c = -2(4\pi^2)$$

In this case the wedge-like region (doubly hatched) of oscillatory instability is in the third quadrant of Figure 6.7.5.

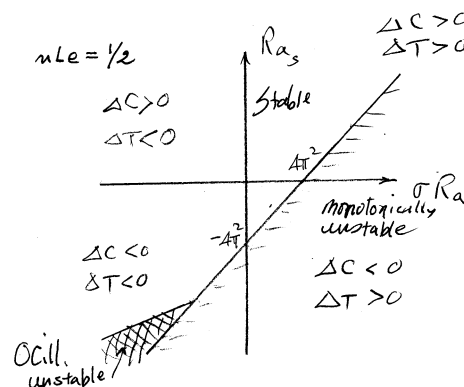


Figure 6.7.5: Domains of stability/instability for $nLe = 1/2$.

6.7.7 Comments on the nonlinear stage

In a Hele-Shaw experiments Griffiths (1981) showed that the monotonic instability leads to fingering. See Figure 6.7.6 for the Hele-Shaw model of fingering in a porous medium Figure

6.7.7 show how the fingers evolve after a long time,

Imhoff & Green have also given laboratory evidence of fingering as a result of such instability as shown in Figure 6.7.8. The mechanism can be of interest in the transport of contaminants in ground water.

6.7.8 Comments on thermalhaline instability in sea water

Motivated by oceanographic interest, Turner has performed laboratory experiments shown in Figure 6.7.10 for more rapidly diffusing salt solution on top of denser sucrose solution. Figure 6.7.10 shows the fingering by pouring hot dilute salt solution on top of a stable temperature gradient.

Unstable growth of the oscillatory instability results in a mixed layer where the salinity and temperature are relatively uniform. At the top of this mixed layer, the salinity is rather discontinuous because of the weak diffusivity. But the temperature profile has a smoother boundary-layer-like transition because of the large diffusivity. The density profile is nevertheless continuous. Now this thermal boundary layer is like a Rayleigh -Benard (or Horton-Rogers-Lapwood) problem. When the jump become large enough the critical Rayleigh number is exceeded so that Benard/Lapwood convection cells appear as sketched in Figure 6.7.11. This process continues until another mixed layer develops. Eventually a staircase profile is developed, as sketched in figure 6.7.12.

Field evidences have been found in oceans where there are strong gradients of temperature and salinity. It has been observed and recorded in Mediteranian Sea "below the warm salty Mediteranian outflow in the eastern North Atlantic and in the western tropical North Atlantic" (Schmitt, 1994). This is reflected by the staircase structure of temperature and salinity profiles, see Figure 6.7.13.

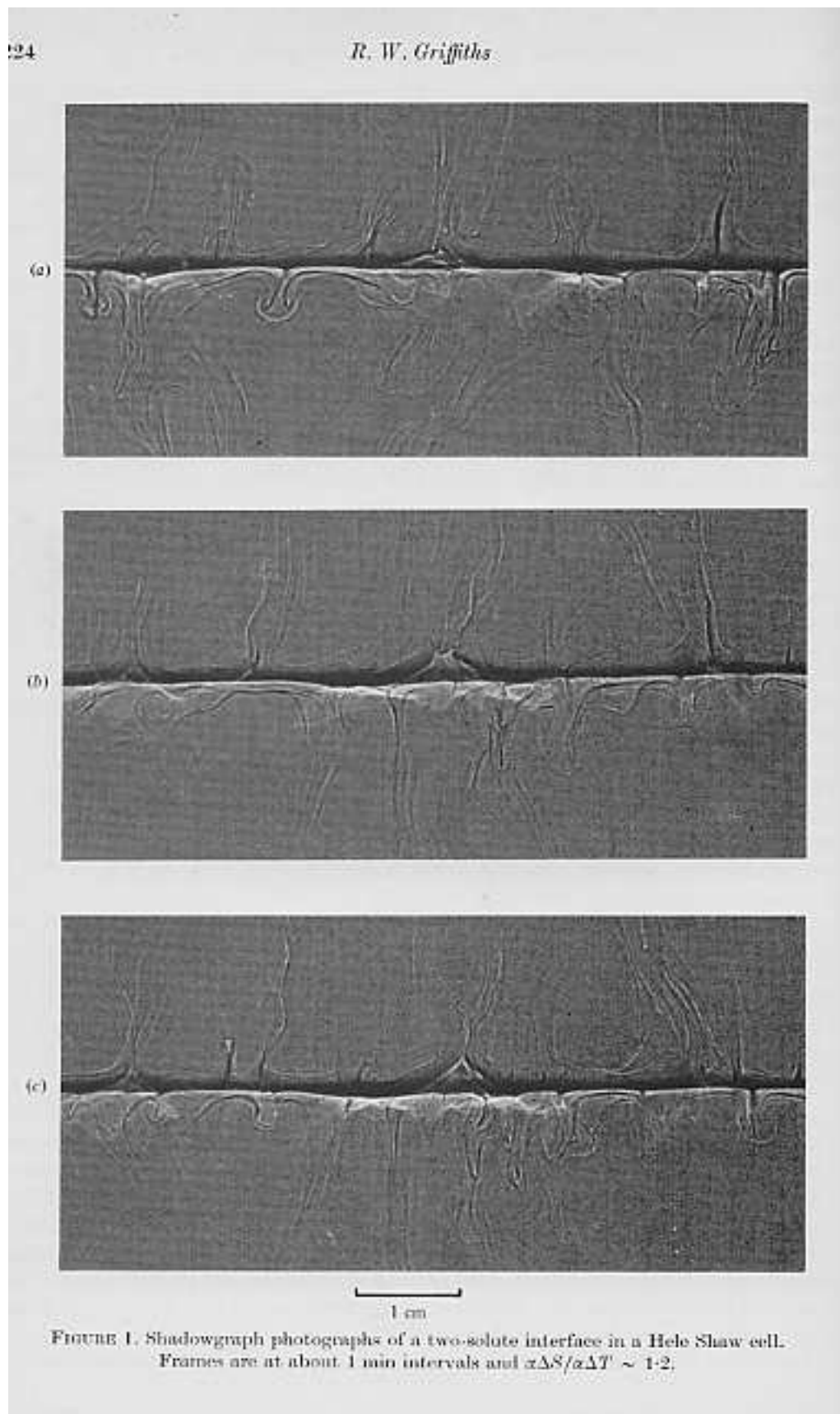


Figure 6.7.6: Development of fingering at the interface of salt/sugar solutions. (Griffiths, 1981)

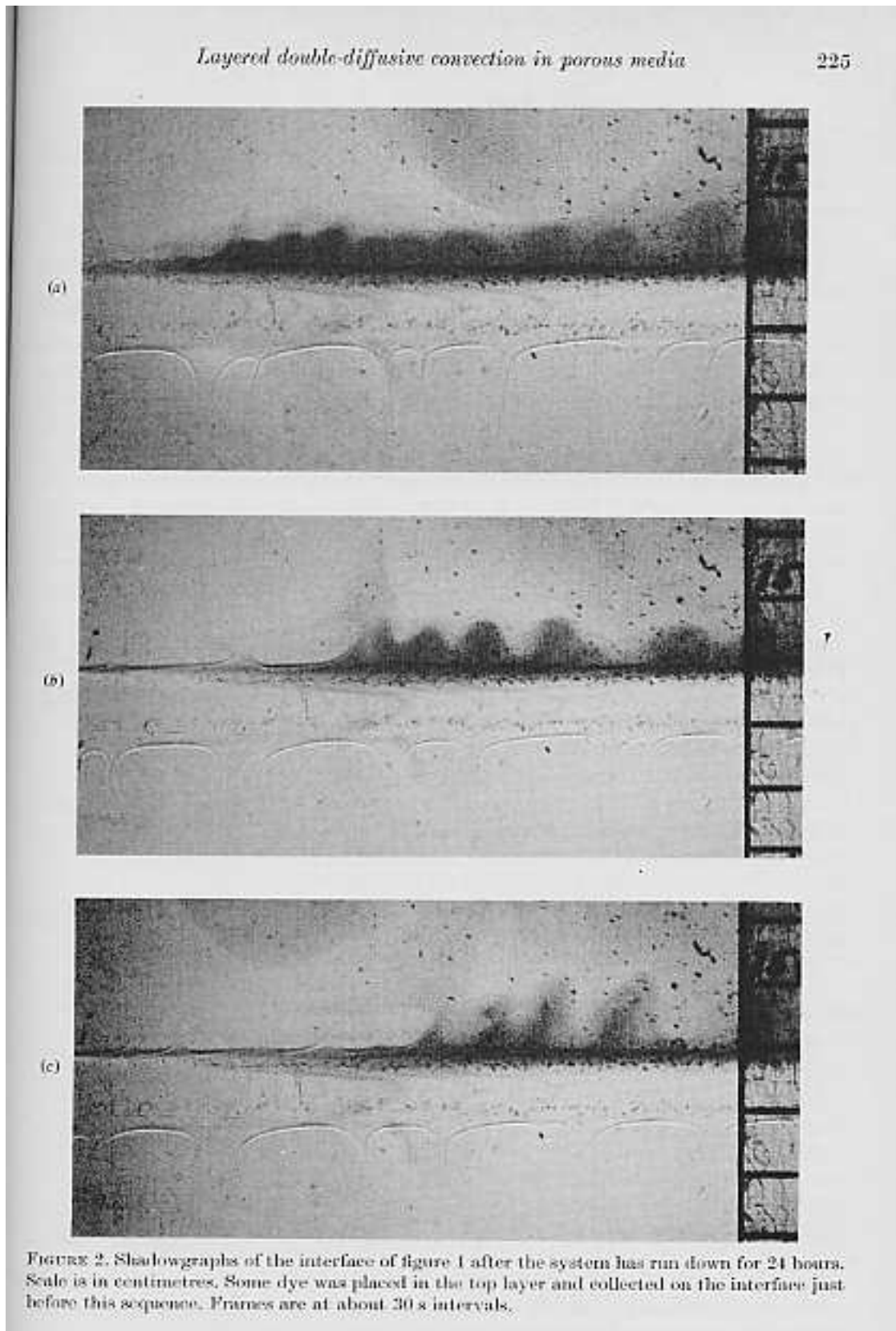


Figure 6.7.7: Development long after fingering at the interface of salt/sugar solutions. (Griffiths, 1981)

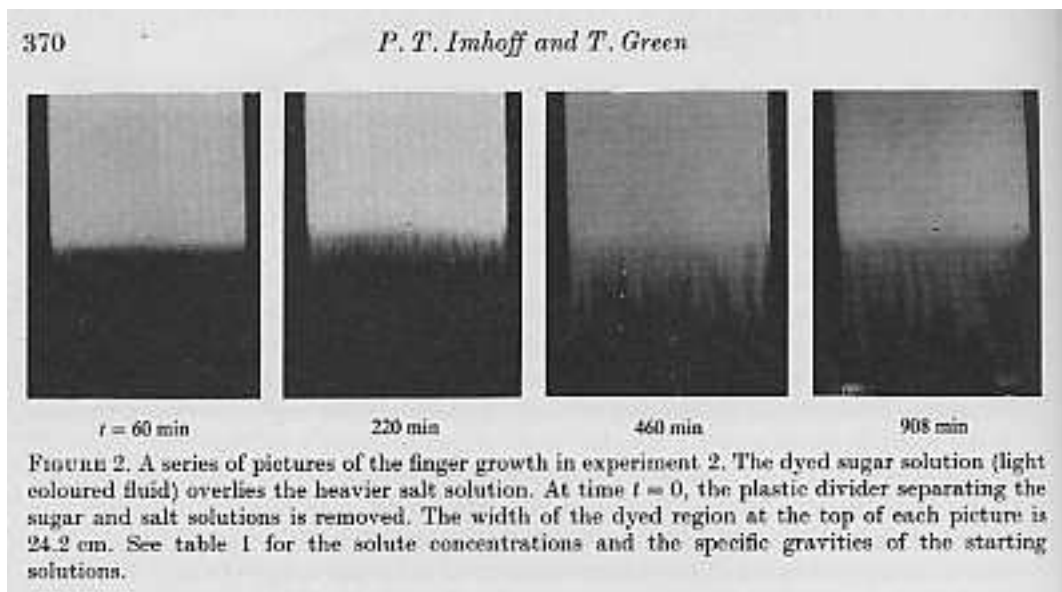


Figure 6.7.8: Fingering at salt/sucrose interface, by Imhoff and Green.

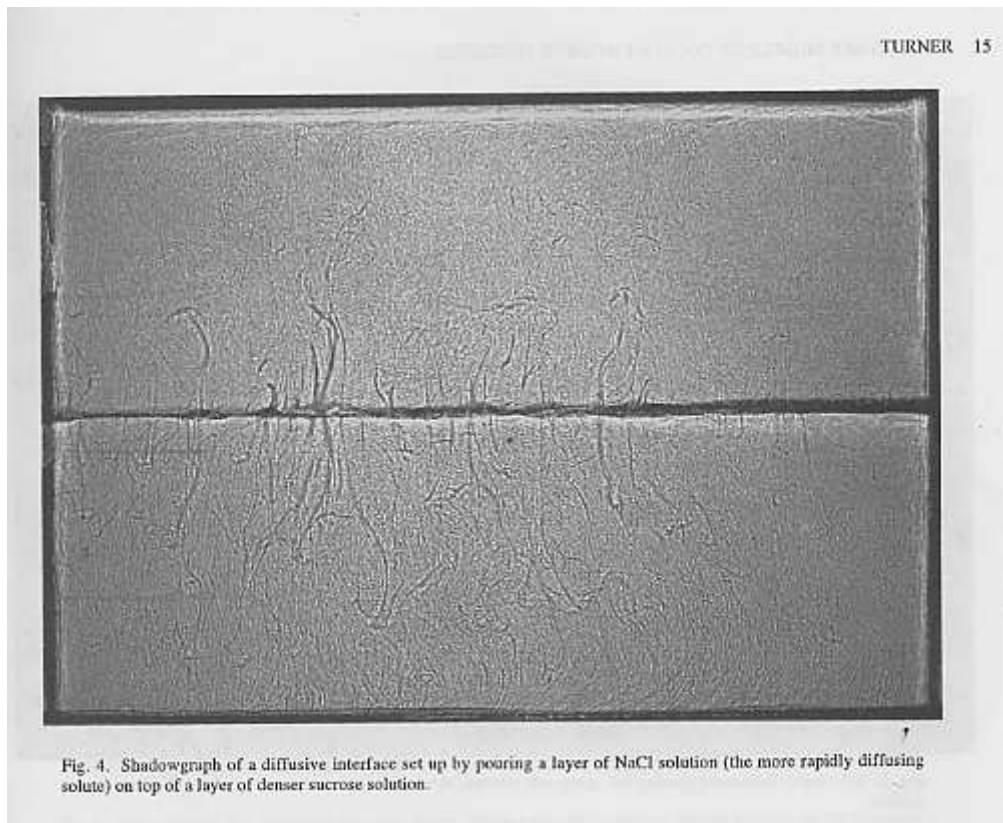


Figure 6.7.9: Fingering along the interface of a salt solution (more diffusive and lighter) on top a sugar solution (less diffusive and heavier). J. S. Turner in *Double Diffusive Convection*, edited by A Brandt and H.J. Fernando, 1995

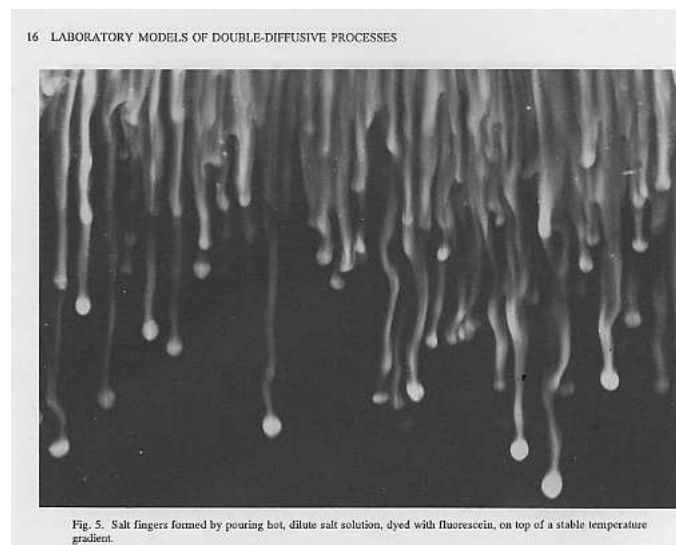


Figure 6.7.10: Fingering due to double-diffusive stability/instability in water. J. S. Turner in *Double Diffusive Convection*, edited by A Brandt and H.J. Fernando, 1995

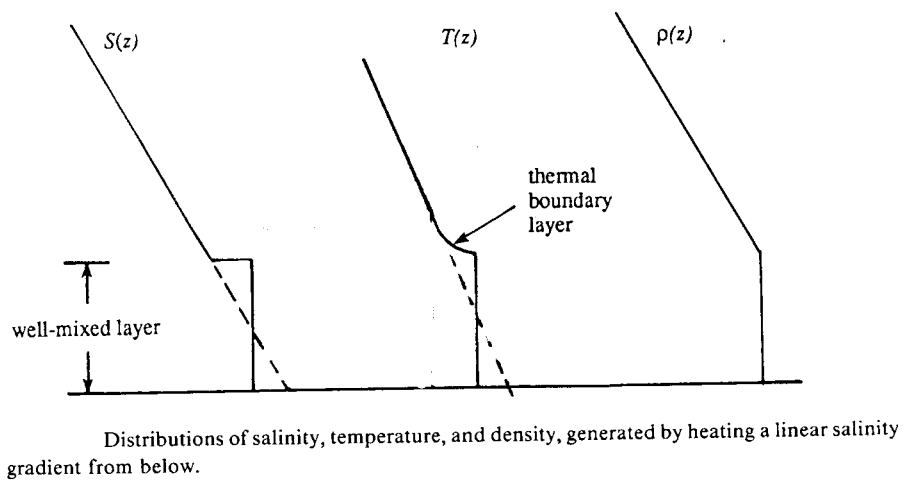


Figure 6.7.11: From Kundu fig 11.9

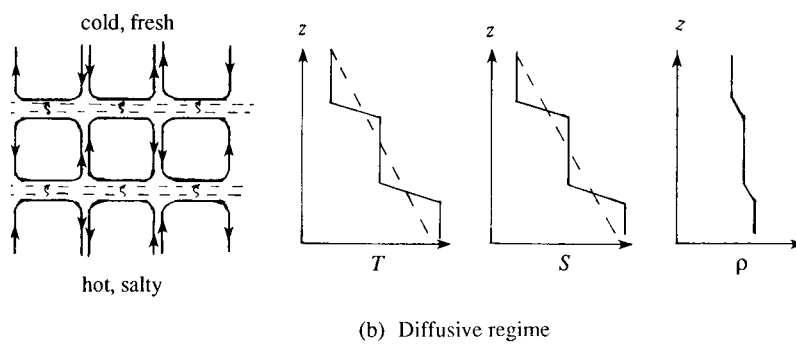


Fig. 11.7 Two kinds of double-diffusive instabilities. (a) Finger instability, showing up- and down-going salt fingers and their temperature, salinity, and density. Arrows indicate direction of motion. (b) Oscillating instability, finally resulting in a series of convecting layers separated by "diffusive" interfaces. Across these interfaces T and S vary sharply, but heat is transported much faster than salt.

Figure 6.7.12: From Kundu, Fig 11.7b

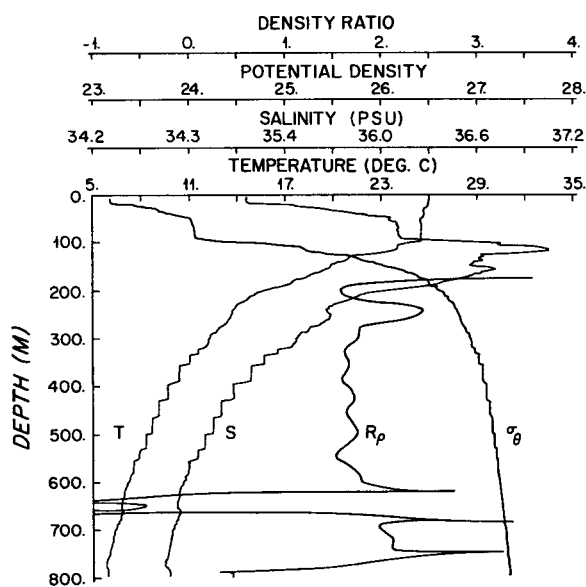


Figure 2 (b) The vertical profiles of temperature, salinity, potential density anomaly (σ_θ , kg/m^3), and R_ρ from a station in the C-SALT area, from the surface to 800 m depth. Temperature contrasts across the steps are typically $0.5\text{--}1.0^\circ\text{C}$. Mixed layers are 5–30 m thick. The layered structure in the 300–600 m depth range has $1.5 < R_\rho < 1.8$.

Figure 6.7.13: Vertical profiles in sea water near Barbados, showing thermohaline staircases (Schmitt, 1994)